Heliyon 10 (2024) e25992

Contents lists available at ScienceDirect

Heliyon

journal homepage: www.cell.com/heliyon

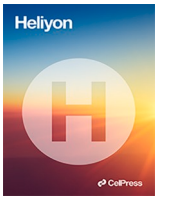

Research article

Suction detection and suction suppression of centrifugal blood pump based on the FFT-GAPSO-LSTM model and speed modulation

Xin Liu [a,b], Hongyi Qu [a,c,*], Chuangxin Huang [a,b], Lingwei Meng [a,b], Qi Chen [a], Qiuliang Wang [a,b,c,**]

[a] Ganjiang Innovation Academy, Chinese Academy of Sciences, Ganzhou, Jiangxi Province, 341000, China
[b] Department of Automation, University of Science and Technology of China, Hefei 230026, China
[c] Institute of Electrical Engineering, Chinese Academy of Sciences, Beijing, 100190, China

ARTICLE INFO

Keywords:
Centrifugal blood pump
Suction detection
Suction suppression
LSTM

ABSTRACT

Centrifugal blood pumps are important devices used to treat heart failure. However, they are prone to high-risk suction events that pose a threat to human health when operating at high speeds. To address these issues, a normal suction detection method and a suction suppression method based on the FFT-GAPSO-LSTM model and speed modulation were proposed. The innovation of this suction detection method lies in the application of the genetic particle swarm optimisation (GAPSO) and the fast Fourier transform (FFT) feature extraction method to the long-term and short-term memory (LSTM) model, thereby improving the accuracy of suction detection. After detecting signs of suction, the suction suppression method designed in this study based on variable-speed modulation immediately takes effect, enabling the centrifugal blood pump to quickly return to its normal state by controlling the speed. The suction detection method was divided into four steps. First, a mathematical model of the coupling of the cardiovascular system and the centrifugal blood pump was established, and a real-time blood flow curve was obtained through model simulation. Second, the signal was preprocessed by adding Gaussian white noise and low-pass filtering to make the blood flow signal close to actual working conditions while retaining the original characteristics. Subsequently, through fast Fourier transform (FFT) analysis of the processed curve, the spectral characteristics that can characterise the working state of the centrifugal blood pump were extracted. Finally, the parameters of the LSTM model were optimised using the GAPSO, and the improved LSTM model was used to train and test the blood flow spectrum feature set. The results show that the suction detection method of the FFT-GAPSO-LSTM model can effectively detect whether centrifugal blood pump suction occurs and has certain advantages over other methods. In addition, the simulation results of the suction suppression were excellent and could effectively suppress the occurrence of suction. These results provide a reference for the design of centrifugal blood pump control systems.

* Corresponding author. Institute of Electrical Engineering, Chinese Academy of Sciences, Beijing, 100190, China.
** Corresponding author. Institute of Electrical Engineering, Chinese Academy of Sciences, Beijing, 100190, China.
E-mail addresses: xliu@gia.cas.cn (X. Liu), quhongyi@mail.iee.ac.cn (H. Qu), cxhuang21@gia.cas.cn (C. Huang), lwmeng20@gia.cas.cn (L. Meng), chenqi@gia.cas.cn (Q. Chen), qiuliang@gia.cas.cn (Q. Wang).

https://doi.org/10.1016/j.heliyon.2024.e25992
Received 30 September 2023; Received in revised form 6 February 2024; Accepted 6 February 2024
Available online 8 February 2024

Abbreviations

LSTM	long-term and short-term memory
GAPSO	genetic particle swarm optimisation
FFT	fast fourier transform
FA	fireworks algorithm
DR	diabetic retinopathy
RNN	Recurrent neural networks
CA	colony algorithm
GA	genetic algorithm
PSO	particle swarm algorithm
kNN	k-Nearest Neighbor

1. Introduction and literature review

1.1. Introduction

According to the clinical data, heart failure has a high mortality rate and is currently the most threatening disease [1–3]. A centrifugal blood pump is the main device employed for treating heart failure. It can assist a damaged heart in pumping blood, thereby solving the problems of insufficient blood pressure and inadequate systemic blood flow perfusion in patients with heart failure [4,5]. However, a fatal flaw can easily occur in the application of centrifugal blood pumps, such as suction [6]. First, we must explain suction. Currently, most centrifugal blood pumps use a constant speed-control method. Notably, in clinical applications, the physiological conditions of patients with heart failure constantly change. When the heart pump speed exceeds the critical speed required for physiological perfusion, the left ventricular pressure decreases and even negative pressure occurs, which is the suction phenomenon. Suction can significantly harm a patient's physical health [7]. Therefore, avoiding suction has become a focus of research on centrifugal blood pumps.

Suction is an instantaneous event without any signs, making it difficult to accurately detect the suction status and respond promptly. However, if not addressed on time, it can have a significant impact on patients with heart failure and even threaten their lives. The suction detection problem of centrifugal blood pumps belongs to state classification, which is the real-time detection of whether the centrifugal blood pump is in a normal or suction state. Therefore, suction detection in centrifugal blood pumps can be achieved using feature extraction and pattern-recognition methods. Suction detection and inhibition are complementary, and only by effectively completing these two tasks can we solve the suction problem of centrifugal blood pumps. As the suction phenomenon is caused by a sudden abnormal high speed of a centrifugal blood pump, suction suppression can be achieved by controlling the speed. For example, using a variable speed strategy, when suction is detected, the speed is quickly reduced until the centrifugal blood pump returns to normal, after which the speed remains unchanged. This variable-speed strategy requires a quick response.

Currently, artificial intelligence is a popular research topic worldwide. Various fields are attempting to employ artificial intelligence. Implantable medical devices, such as classification and recognition technologies in artificial intelligence, can effectively solve the problem of suction detection in centrifugal blood pumps [8,9]. A BP neural network is a multilayer feedforward network trained based on an error-backpropagation algorithm, which is the most widely used algorithm for classification recognition and prediction [10]. This can achieve nonlinear mapping, has self-learning ability, and can be generalised. However, the shortcomings of BP neural networks are also evident, such as slow speed, possibility of entering local minima and training failure, and susceptibility to underlearning or overlearning. A support vector machine (SVM) is also a common classification and recognition algorithm that uses kernel functions instead of high-dimensional mapping, which can propose larger samples, and therefore has less robustness [11]. The disadvantage of the SVM is that it cannot easily implement large-scale training and has great difficulties in solving multiple classifications. Recurrent neural networks (RNNs) are a type of artificial intelligence that possess a self-learning ability, high memory capacity, and the ability to quickly train and optimise [12,13]. Moreover, RNNs have significant advantages in training the nonlinear features of sequences and image processing. Coincidentally, when a centrifugal blood pump is used for suction detection, many blood flow images and nonlinear features must be trained. Therefore, compared to BP neural networks and SVM, RNNs are more suitable for suction detection in centrifugal blood pumps. For suction detection in centrifugal blood pumps, the sample feature size can be calculated using a fast Fourier transform (FFT) and then trained and tested using an RNN [14]. However, traditional RNNs have the disadvantage of long-term dependence, which can lead to a low accuracy of suction detection. The generation of long-short-term memory (LSTM) compensates for the aforementioned shortcomings [15]. LSTM is an improved recurrent neural network (RNN) algorithm. Because of its strong training ability and high accuracy, it is widely used in state detection and classification recognition.

Owing to many parameters in the LSTM model, it is often difficult to achieve global optimisation or even overfitting, owing to improper parameter selection. Intelligent optimisation algorithms can effectively compensate for the aforementioned shortcomings by optimising the parameters. The commonly used optimisation algorithms include the artificial ant colony algorithm (CA) [16], genetic algorithm (GA) [17], firework algorithm (FA) [18], and particle swarm optimisation (PSO) algorithm [19]. The PSO algorithm has a simple structure and good optimisation performance. Therefore, the PSO algorithm is widely used in various applications. Genetic algorithm PSO (GAPSO) is an improved PSO algorithm that combines the advantages of the GA and PSO, and can overcome the

shortcomings of the traditional PSO such as low efficiency and ease of falling into local optima [20].

Based on the analysis, this study proposes a centrifugal blood pump suction detection and suction suppression method based on FFT-GAPSO-LSTM. In Section 2, the research object is introduced, and a coupling model between the cardiovascular and centrifugal blood pumps is established. Based on this model, the real-time blood flow curve of the centrifugal blood pump is simulated using MATLAB/Simulink software. In Section 3, the basic theories of FFT analysis, GAPSO optimisation, and LSTM prediction methods are introduced, and a centrifugal blood pump suction-detection model based on the FFT-GAPSO-LSTM model is established. In Section 4, a detection model is used to preprocess, extract features, and train the blood flow dataset. In Section 5, suction suppression methods designed for potential suction occurrences are described. Finally, Section 6 provides a summary and outlook.

1.2. Literature review

With the development of the signal-processing technology and classification recognition algorithms, an increasing number of fields are using a combination of feature extraction and pattern recognition to complete fault diagnosis, state classification, and event prediction [21–24]. Suction is no exception. In recent years, many studies have reported on the relevant content. Reference [25] reported a suction-detection method based on sensorless control and verified its feasibility through animal experiments; however, the detection accuracy requires further improvement. Reference [26] proposed a method for preventing suction that considered whether the minimum left ventricular pressure was lower than 1 mmHg as the standard for determining whether suction occurred when designing a controller [26]. However, this increases the amount of control and complicates the control systems. Moreover, a detailed suction detection plan was not clearly provided in Ref. [26]. Therefore, after completing suction detection, a suction-detection method based on speed modulation to suppress possible suction must be designed. Reference [27] proposed an RNN-LSTM model for testing the diabetic retinopathy (DR) classification model. The test results of 2500 data points indicated that the classification model could effectively identify the five types of DR. In addition, the RNN-LSTM model was compared with the SVM in the literature to verify the superiority of this model. Reference [28] reported a robust hybrid classification model based on population optimisation, which included the flower pollination algorithm (FPA), support vector machine (SVM), and convolutional neural network (CNN). The disease classification of apple, grape, and tomato plants was completed through feature extraction, parameter optimisation, and clustering analysis, and the effectiveness of the method was verified experimentally. Reference [29] reported a DR classification method based on a GA and a k-Nearest Neighbor (kNN) model and compared this method with Gaussian Naive Bayes. The results indicated that the kNN model had high accuracy and excellent classification performance, which are important for the early diagnosis of DR. These methods are applications of various classification and detection methods in various aspects and have all achieved good results. Methods applicable to each field differ, and finding a suitable method is crucial.

The LSTM model is a special type of recurrent neural network, characterised by its ability to retain useful historical information over a long time [30,31]. Reference [32] solved the detection and classification problem of urban transportation modes using an LSTM model with a detection accuracy of up to 98%. Reference [33] designed an LSTM model for the seizure detection of epileptic diseases, and the results showed that after training, the classification accuracy of epileptic and non-epileptic seizures was 99.5%, indicating that the LSTM model had a good classification effect. Reference [34] proposed an LSTM neural network model for travel time prediction and predicted the multistep forward time of each link through training and testing. The results indicated that the model had a high prediction accuracy. For the state classification and suction detection of centrifugal blood pumps, the LSTM model is undoubtedly the most suitable because it excels in processing the blood flow characteristics that can characterise the state of the centrifugal blood pump.

2. Research object and modelling

2.1. Research object

The research object of this study was a magnetic levitation centrifugal blood pump independently developed by our laboratory. The structure of the heart pump is shown in Fig. 1 [4,5,20]. Among them, Fig. 1 (a) is the model diagram, and Fig. 1 (b) is the object picture.

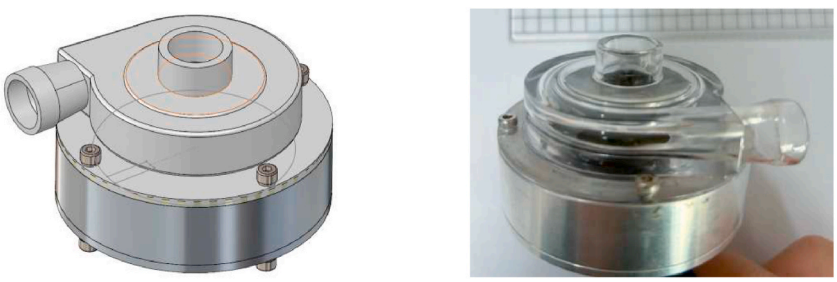

(a) (b)

Fig. 1. Structure diagram of the heart pump: (a) model diagram; (b) object picture.

The specific geometric parameters of the blood pump are as follows: the overall outer diameter is 50 mm, overall axial length is 23.2 mm, pump casing diameter is 46 mm, impeller outer diameter is 32 mm, blade outlet width is 4.71 mm, and number of blades is six. The outer shell of the centrifugal pump was made of a transparent material, which enabled a more intuitive observation of the rotation of the impeller and flow characteristics of blood inside the centrifugal pump during the experiments.

2.2. Coupling model of the cardiovascular system and centrifugal blood pump

Combining the basic knowledge of the cardiovascular system and centrifugal blood pump [5], a coupling model between the cardiovascular system and centrifugal blood pump was established using the electrical network equivalence theory, as shown in Fig. 2.

As shown in Fig. 2, the left atrium, left ventricle, aorta, artery, systemic circulation, right atrium, right ventricle, pulmonary artery, pulmonary circulation, and pulmonary vein are in a clockwise direction. The path in the upper part represents the left heart and systemic circulation. The elliptical dotted line represents the heart pump, which is connected in parallel between the left ventricle and the aorta, while the lower part represents the right heart and pulmonary circulation. Among them, $P_{la}(t)$, $P_{lv}(t)$, $P_{ao}(t)$, $P_{sar}(t)$, $P_{sv}(t)$, $P_{ra}(t)$, $P_{rv}(t)$, $P_{pa}(t)$, $P_{par}(t)$, and $P_{pv}(t)$ indicate the blood pressure of the left atrium, left ventricle, aorta, artery, systemic circulation, right atrium, right ventricle, pulmonary artery, pulmonary circulation, and pulmonary vein, respectively. $C_{la}(t)$, $C_{lv}(t)$, $C_{ao}(t)$, $C_{sar}(t)$, $C_{sv}(t)$, $C_{ra}(t)$, $C_{rv}(t)$, $C_{pa}(t)$, $C_{par}(t)$, and $C_{pv}(t)$ indicate compliances of the left atrium, left ventricle, aorta, artery, systemic circulation, right atrium, right ventricle, pulmonary artery, pulmonary circulation, and pulmonary vein, respectively. The vascular wall is elastic, and compliance is used to indicate the degree of change in the vascular volume with changes in blood pressure. Diodes D_{mv}, D_{av}, D_{tv}, and D_{pv} represent the mitral, aortic, tricuspid, and pulmonary valves, respectively, and their conduction and cut-off represent valve opening and closing, respectively. R_{mv}, R_{av}, R_{ao}, R_{svr}, R_{sv}, R_{tv}, R_{pv}, R_{pa}, R_{pvr}, and R_{pv} are mitral valve flow resistance, aortic valve flow resistance, aortic flow resistance, systemic circulation peripheral resistance, systemic circulation venous resistance, tricuspid valve flow resistance, pulmonary valve flow resistance, pulmonary artery flow resistance, pulmonary circulation peripheral resistance, and pulmonary circulation venous resistance, respectively. L_{ao} and L_{pa} represent the blood inertia of the aorta and pulmonary arteries, respectively.

The model was built using MATLAB/Simulink. The sampling period was set at 0.001 s, and the simulation time was set at 60 s. First, we simulated the haemodynamic curves (blood pressure and blood flow) under normal conditions, as shown in Fig. 3. Subsequently, the speed of the centrifugal blood pump was increased linearly from 4000 r/min to 9500 r/min until suction occurred, as shown in Fig. 4.

The aortic pressure curve in Fig. 3 (a) shows that the aortic pressure of patients with heart failure was maintained between 81 and 124 mmHg under the normal assistance of the centrifugal blood pump. This range is close to the aortic pressure range of a normal heart, indicating that the cardiovascular system and centrifugal blood pump coupling model established in this study are effective in simulating the physiological state and haemodynamic information of the human body. Fig. 3 (b) shows the blood-flow curve of the

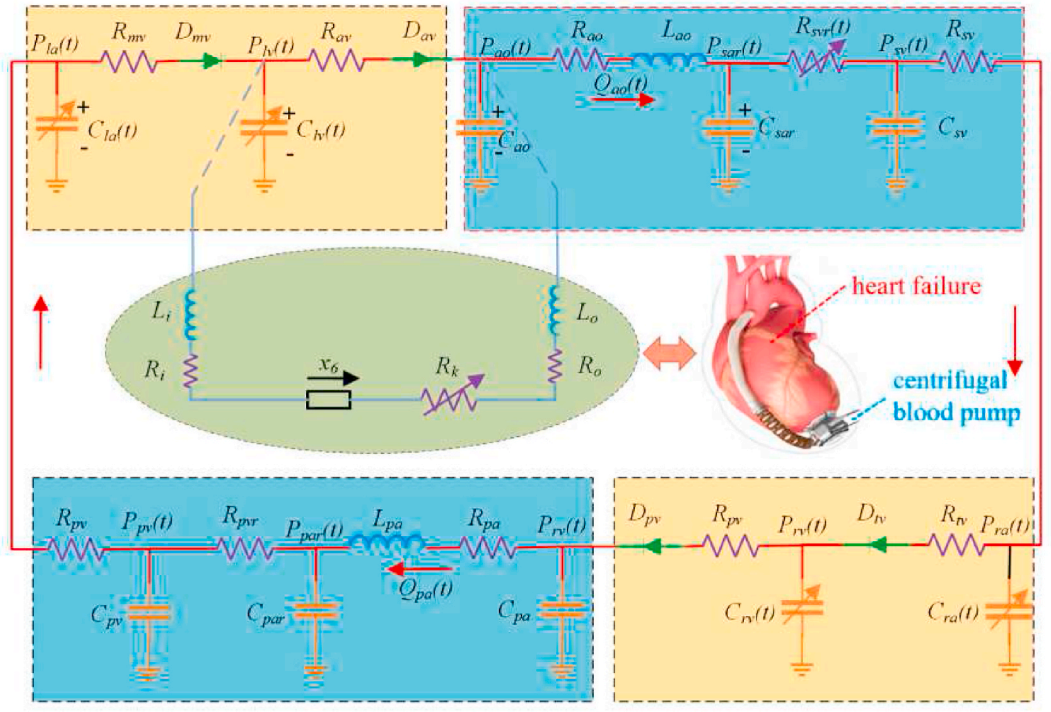

Fig. 2. Schematic diagram of the control system.

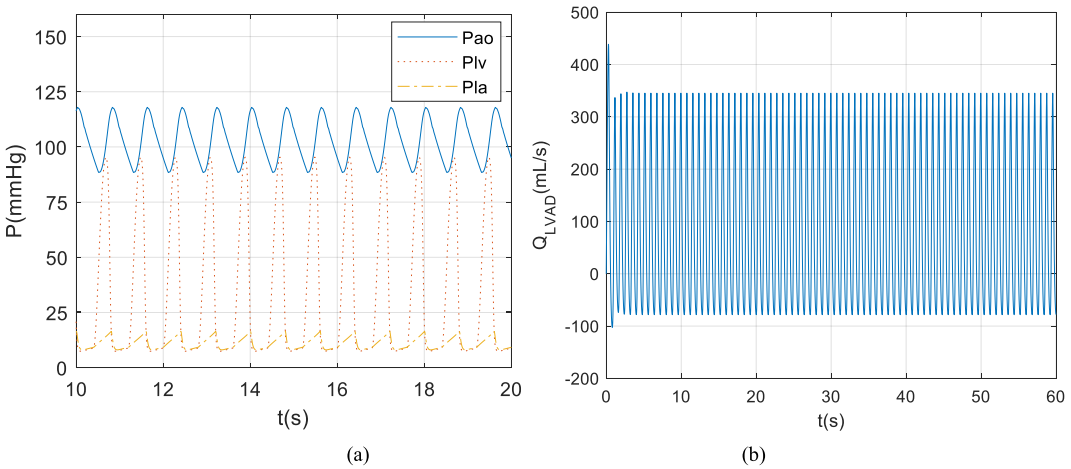

Fig. 3. Hemodynamic curves: (a) blood pressure curve (intercept the results of 10s–20s); (b) blood flow curve.

extracardiac blood pump under normal auxiliary conditions. The blood flow changes in a periodic symmetry under normal conditions, and its frequency of change is synchronized with the beating of the heart, thereby assisting the damaged heart in satisfying the systemic blood perfusion requirements.

Fig. 4 (a) shows a linear change in the speed of the centrifugal blood pump during suction. When the speed increased linearly to the critical value, sudden suction occurred. Fig. 4 (b) shows the blood-flow curve of the centrifugal blood pump during suction. As the rotational speed increased, the amplitude of blood flow in the centrifugal blood pump decreased. This phenomenon also indicates that the blood pulsatility of the centrifugal blood pump decreases with an increase in the rotational speed. Suction occurred when the speed reached a critical value. At this point, the changes in blood flow became disordered, and the amplitude increased. Most importantly, when suction occurred, the periodic symmetry of the blood flow also disappeared.

Comparing the blood flow curves in Fig. 3 (b) and Fig. 4 (b), the blood flow characteristics under normal and aspirated conditions are significantly different, which provides a possibility for designing subsequent suction-detection methods. The two blood flow signals obtained in this section provide data samples for the LSTM neural network model.

3. Research method design

The suction-detection model designed in this study involved the FFT, GAPSO, and LSTM models. The basic principles and structures of the three methods are elaborated in this section, and an FFT-GAPSO-LSTM suction-detection model is designed based on these methods.

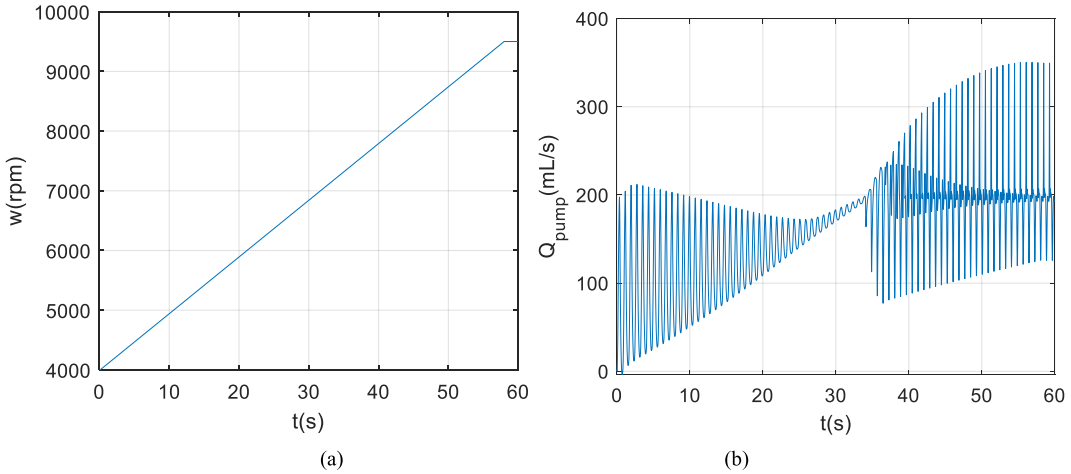

Fig. 4. Result when suction occurs: (a) rotor speed curve; (b) blood flow curve before and after suction.

3.1. FFT method design

According to the basic Fourier transform principles, it is easy to obtain the formula for the discrete Fourier transform as follows [35]:

$$\begin{cases} Z(k) = \sum_{n=0}^{N-1} z(n) W_N^{kn} \\ W_N = e^{-j\frac{2\pi}{N}} \end{cases} \tag{1}$$

where, $n = 0, 1, \ldots, N-1$; $k = 0, 1, \ldots, N-1$; $Z(k)$ represents the signal processed using the discrete Fourier transform, $z(n)$ represents the sampled signal, and W represents the unit vector.

As a fast algorithm for the discrete Fourier transform, FFT has the advantages of fast computation and high efficiency. Therefore, in this study, the FFT was used to extract the frequency-domain features of the blood flow signal of a centrifugal blood pump. To improve efficiency, the sampled signals $z(n)$ were decomposed into odd sequences $z_1(n_1)$ and even sequences $z_2(n_2)$ by FFT during signal processing. The formula used is as follows [36]:

$$z(n) = z_1(n_1) + z_2(n_2) \tag{2}$$

where n_1 and even number, n_2 is and odd numbers, respectively, and the sequence lengths of $z_1(n_1)$ and $z_2(n_2)$ are equal ($N/2$).

Furthermore, the FFT formula is obtained as follows [37]:

$$Z(k) = \sum_{n=0}^{\frac{N}{2}-1} z_1(n_1) W_{\frac{N}{2}}^{kn} + W_N^{kn} \sum_{n=0}^{\frac{N}{2}-1} z_2(n_2) W_{\frac{N}{2}}^{kn} = Z_1(k) + W_N^{kn} Z_2(k) \tag{3}$$

where, $Z_1(k)$ and $Z_2(k)$ are the discrete Fourier transforms of $z_1(n_1)$ and $z_2(n_2)$.

3.2. LSTM neural network

The LSTM neural network is a type of RNN and can also be considered an improved RNN algorithm. Because traditional RNNs only have one internal state and suffer from long-term dependency on relational models during training, RNNs may not handle long-term sequences effectively. The LSTM neural network overcomes these limitations because it can achieve self-assessment and has certain advantages in solving long-interval sequences and classification detection problems [38]. The LSTM neural network consists of four progressive network layers, and its structural schematic is shown in Fig. 5. LSTM neural networks have unique long- and short-term memory mechanisms, including short-term memory h and long-term memory C. Extensive training is performed using LSTM neural networks to ensure the system's long-term memory of effective signals or data. In addition, the setting of three gate structures (forgetting gate, input gate, and output gate) in the LSTM neural network makes the addition, elimination, and updating of data more efficient.

where f_t、i_t、o_t represents the forgetting, input, and output gates, respectively; C_t、h_t represents the neural unit state and hidden layer state at time t; and σ、tanh represents the activation function.

As shown in Figure (5), the LSTM neural network sets the forgetting, input, and output gates for each state at each moment. The forget gate is a summary of the information quantity of the elements whose states were ignored in the previous moment and saved in the current state. The input gate inputs the data transmitted by the preamble module into long-term state C, which represents most of the information stored in the system. The output gate performs output processing in the long-term state after processing, which is determined by the previous state output and current state input. The mathematical relationship between the two is as follows [38]:

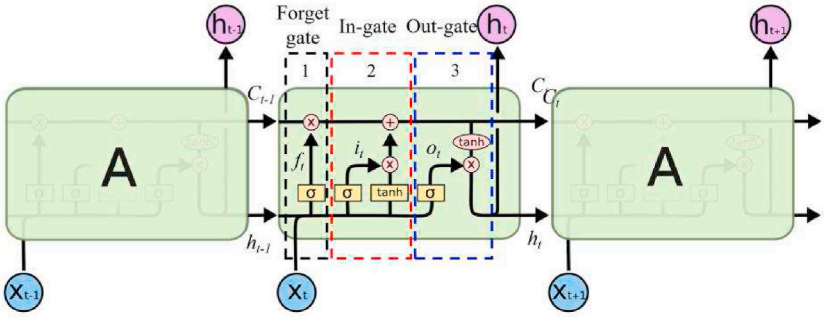

Fig. 5. Structural schematic diagram of the LSTM neural network.

$$
\begin{aligned}
f_t &= \sigma\left(W_f \cdot [h_{t-1}, x_t] + b_f\right), \\
i_t &= \sigma(W_i \cdot [h_{t-1}, x_t] + b_i), \\
o_t &= \sigma(W_o \cdot [h_{t-1}, x_t] + b_o), \\
C_t &= \tanh(W_C \cdot [h_{t-1}, x_t] + b_C), \\
C_t &= f_t * C_{t-1} + i_t * C_t, \\
h_t &= o_t * \tanh(C_t)
\end{aligned} \tag{4}
$$

In Equation (4), W represents the weight; the weights of each part are different, and b represents the offset of each part.

From Equation (4), it can be observed that the LSTM model has many parameters, and the summarised initialisation parameters are shown in Table 1.

Because LSTM neural networks are prone to poor training performance owing to improper settings of the number of hidden layer units and learning rate, manual parameter tuning or relying on expert experience can lead to low efficiency and difficulty in achieving global optimisation. The PSO algorithm can effectively solve these problems by optimising the parameters.

3.3. GAPSO optimisation algorithm

Before introducing the genetic particle swarm algorithm, the particle swarm algorithm is briefly introduced. PSO is a biological heuristic optimisation algorithm based on the clustering activities of birds. Compared with optimisation algorithms such as the ant CA, immune optimisation algorithm, and GA, the PSO algorithm has strong memory, fast convergence speed, and high efficiency. Therefore, it is suitable for optimising the parameters of LSTM neural networks.

The iterative formula of the traditional PSO is [39]:

$$
V_p^{k+1} = \omega V_p^k + c_1 r_1 \left(W_p - X_p^k\right) + c_2 r_2 \left(W_g - X_p^k\right) \tag{5}
$$

$$
X_p^{k+1} = X_p^k + V_p^{k+1} \tag{6}
$$

where Xp and Vp are the position and velocity of the pth particle in the particle swarm, respectively; Wp is the position of the pth particle in the particle swarm when it reaches the optimal position; Wg represents the position when the entire particle swarm reaches the optimal position; k is the number of iterations; ω is the particle inertia weight; c_1、c_2 is the learning factor; and r_1、r_2 is a random number in [0 1].

To improve the optimisation performance of PSO, improve its poor convergence performance, and prevent it from falling into a local optimum, this study introduces an improvement algorithm that integrates the genetic algorithm and PSO. Subsequently, the GAPSO algorithm is applied to LSTM neural networks, which can improve the performance of PSO and overcome the defects of poor convergence performance and ease of falling into the local optimum.

In a previous study, we simulated and verified the superiority of the GAPSO algorithm. Several different PSO algorithms were used to optimise the commonly used test functions, and Fig. 6 shows the results of the previous tests.

As shown in Fig. 6, it is easy to conclude that the convergence performance of the GAPSO algorithm is the best, and its efficiency is dozens of times that of the other two PSO algorithms, indicating that it is more flexible and less prone to falling into local optima. Therefore, this study uses the GAPSO algorithm to optimise the parameters of the LSTM neural network.

3.4. A centrifugal blood pump suction-detection method based on the FFT-GAPSO-LSTM model

Based on the introduction of the FFT method, LSTM neural network, and GAPSO algorithm, combined with the basic principles of the signal preprocessing and FFT analysis methods, a centrifugal blood pump suction-detection method based on the FFT-GAPSO-LSTM model can be designed. A schematic of this process is shown in Fig. 7.

Fig. 7 shows that although the proposed model may appear complex, each part plays its own role. Therefore, the execution efficiency of the model was high, particularly after GAPSO optimisation. This is because the parameters were uncertain before the

Table 1
State variables in the combined the cardiovascular system model.

Parameters of the LSTM model	Initial value
The initialize weights	[-0.5,0.5]
b_f	1 or 2
b_i	[0,0.8]
b_o	[0,0.8]
Iterations	100
Population size	50
Learning factor (c_1)	1.5
Learning factor (c_2)	1.7
Number of hidden layer units (m)	100
Learning rate (r)	0.01

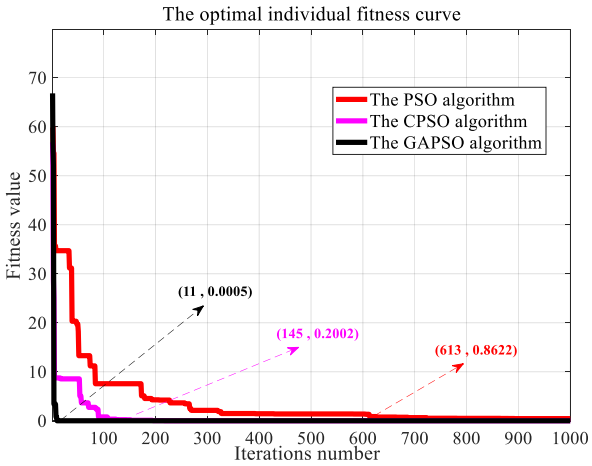

Fig. 6. Convergence comparison of several kinds of PSO algorithms.

parameter optimisation. The steps summarising the suction detection method based on the schematic diagram are as follows:

(1) Signal preprocessing. First, Gaussian white noise signals were added to the blood flow signals obtained from the simulation of the different states in Section 2 to accurately reflect the possible noise interference that the centrifugal blood pump may experience during actual operation. Based on the research results in Ref. [40], the signal-to-noise ratio of a Gaussian white noise signal was set to 20 dB. Subsequently, to reduce the impact of adding a Gaussian white noise signal to the system, a low-pass filtering command was applied to the signal after adding the Gaussian white noise signal. The preprocessed signal can better represent the blood flow information in a human physiological environment.

(2) An FFT analysis was used to convert the preprocessed blood flow time-domain signal into a frequency-domain signal, and the amplitude–frequency characteristics of the frequency-domain signal were extracted. The sampling frequency of the blood flow signal was set to fs = 100 Hz.

(3) The LSTM model was constructed as described in Section 2.2. The existing LSTM method was improved as follows: As the LSTM model does not have the function of detection and classification, this study adds a softmax function layer and a classification Layer to the model to help provide two outputs: the normal state and suction state. Subsequently, as described in Section 2.3, a GAPSO algorithm was designed and used to optimise the parameters of the LSTM model. When optimising the parameters, the number of hidden layer units m and learning rate r were placed as particles in the GAPSO algorithm for optimisation, and the

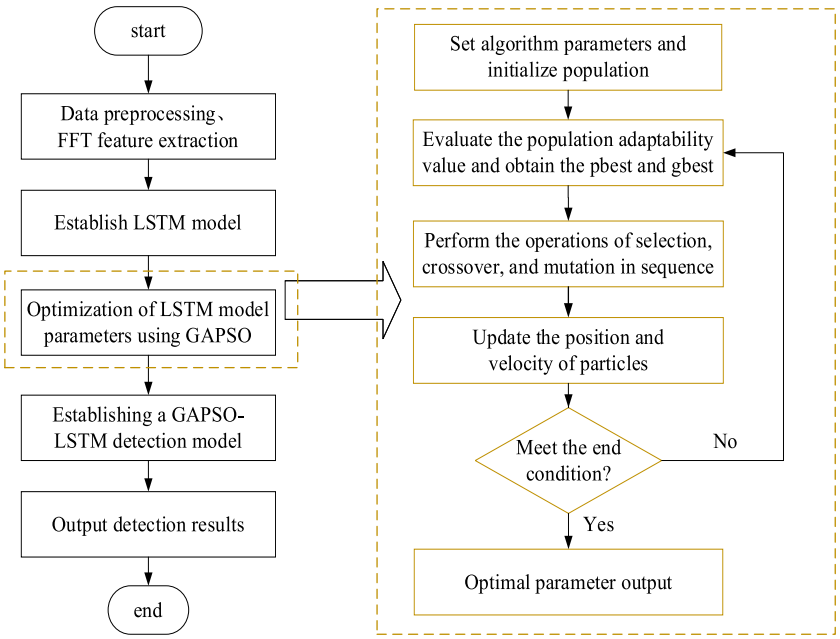

Fig. 7. The schematic diagram of the centrifugal blood pump suction detection method based on the FFT-GAPSO-LSTM model.

optimisation termination condition was set to 200 iterations. After parameter optimisation using the GAPSO algorithm, the optimal values for the number of hidden layer units m and learning rate r were 58 and 0.0022, respectively. The contributions of this improvement include achieving automatic parameter optimisation and improving the model detection accuracy.

(4) The feature signals obtained in Step (2) were used as the training set for the FFT-GAPSO-LSTM model. After completing the model training, several sets of blood flow signals were resimulated and used as the testing set to test the accuracy of detecting the state of the centrifugal blood pump.

4. Results and analysis of suction detection

4.1. Feature extraction results

This method must be tested for verification. Following the steps of the suction-detection method described in Section 2.4, the signal-to-noise ratio and low-pass filter processing were first added to the blood flow signals in different states. After preprocessing the blood flow signal, an FFT analysis was used to convert the preprocessed time domain signal into a frequency domain signal, and the amplitude–frequency characteristics of the frequency-domain signal were extracted. The feature extraction results are shown in Fig. 8.

Fig. 8(a) shows the blood flow diagram and corresponding frequency characteristic diagram of the off-heart blood pump under normal conditions. Fig. 8(b) shows the blood flow diagram and corresponding frequency characteristic diagram under normal conditions. The fundamental, 20th-order, and 39th-order frequencies are more prominent in the amplitude–frequency characteristics of blood flow under normal conditions, and their frequencies are much higher than those of other frequencies. In the case of suction, the fundamental frequency and 41st-order frequency were more prominent. In addition to the two prominent frequencies, the values of the other frequencies in the suction state were higher than those in the normal state. Therefore, a significant difference exists in the frequency changes corresponding to the FFT transformation between the normal and suction states, which can be input as a feature quantity into the LSTM model for training.

Fig. 8 shows the results for only one working condition. Many blood flow charts and corresponding FFT frequency characteristic maps can be obtained under different operating conditions. These frequency features serve as a sample set for the LSTM model. The trained LSTM model will gain a suction-recognition ability, which means that the amplitude–frequency characteristics can be quickly identified for any blood flow curve and then determine whether the centrifugal blood pump is in a normal or suction state.

4.2. Training and testing

The LSTM model requires big blood flow curve data for training, and the training effect must be tested after training with minimal data support. Therefore, MATLAB/Simulink was used for the batch simulation of the normal and suction states, and 4,000 blood flow

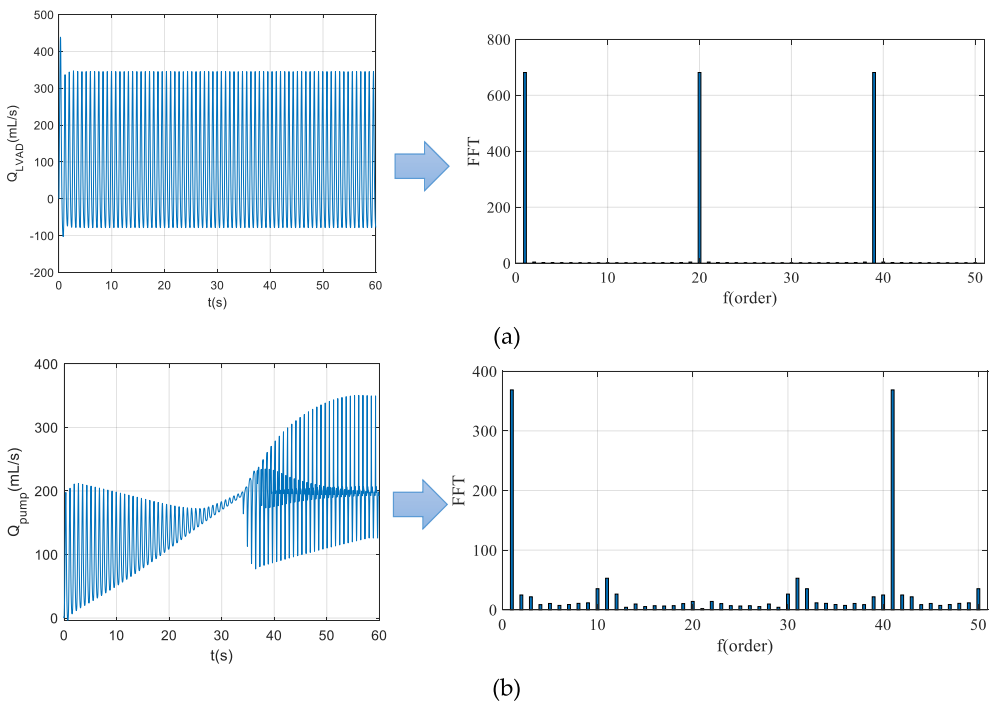

Fig. 8. Feature extraction results: (a) normal state; (b) suction state.

data points from the centrifugal blood pump were obtained. Among them, 3,600 data points were used for model training, and the remaining 400 data points were used for effect testing. The maximum number of iterations of the LSTM network was set to 100. The parameter settings of the LSTM model are listed in Table 1, except for the number of hidden layer units *m* and the learning rate *r*. These two parameters were optimised using the GAPSO algorithm with values of 58 and 0.0022, respectively. The results of training and testing are shown in Fig. 9.

Fig. 9 shows that the improved LSTM model performed well in suction detection. Fig. 9 (a) shows the changes in the accuracy and loss functions of the training set during the training process. As the number of iterations increased, the accuracy of the model rapidly increased and the model loss rapidly decreased. After only nine iterations, the accuracy of the model reached 100%, and the corresponding loss decreased to zero, indicating that the iterative performance of the detection model was excellent.

Fig. 9 (b) shows the confusion matrix of the suction detection results after training with big blood flow curve data. Among these samples, 1,750 normal and 1,850 suction states were detected. The FFT-GAPSO-LSTM model designed in this paper has an overall detection accuracy of 100% for different states of centrifugal blood pumps. This detection accuracy is extremely high and satisfies the practical application requirements for centrifugal blood pump suction detection.

Fig. 9 (c) shows the test effect diagram. By testing 400 blood-flow simulation data points, the trained LSTM model can still achieve 100% detection accuracy when applied to new data. There were no instances of misjudgement in either the training or test results. The analysis verified the effectiveness of the FFT-GAPSO-LSTM model, indicating that it can achieve real-time detection of the status of centrifugal blood pumps.

4.3. Comparative analysis

To further verify the superiority of the FFT-GAPSO-LSTM model in suction detection, FFT-LSTM, FFT-PSO-LSTM, FFT-APSO-LSTM, BP neural network, and SVM models were established for comparison. The BP neural network and SVM were selected as comparative items because they are the most commonly used methods in the field of classification recognition and detection and have strong representativeness. The FFT-LSTM, FFT-PSO-LSTM, and FFT-APSO-LSTM models were used as comparative items to verify the superiority of the GAPSO algorithm for optimising the parameters of the FFT-LSTMl model.

The parameter configurations for each method are as follows:

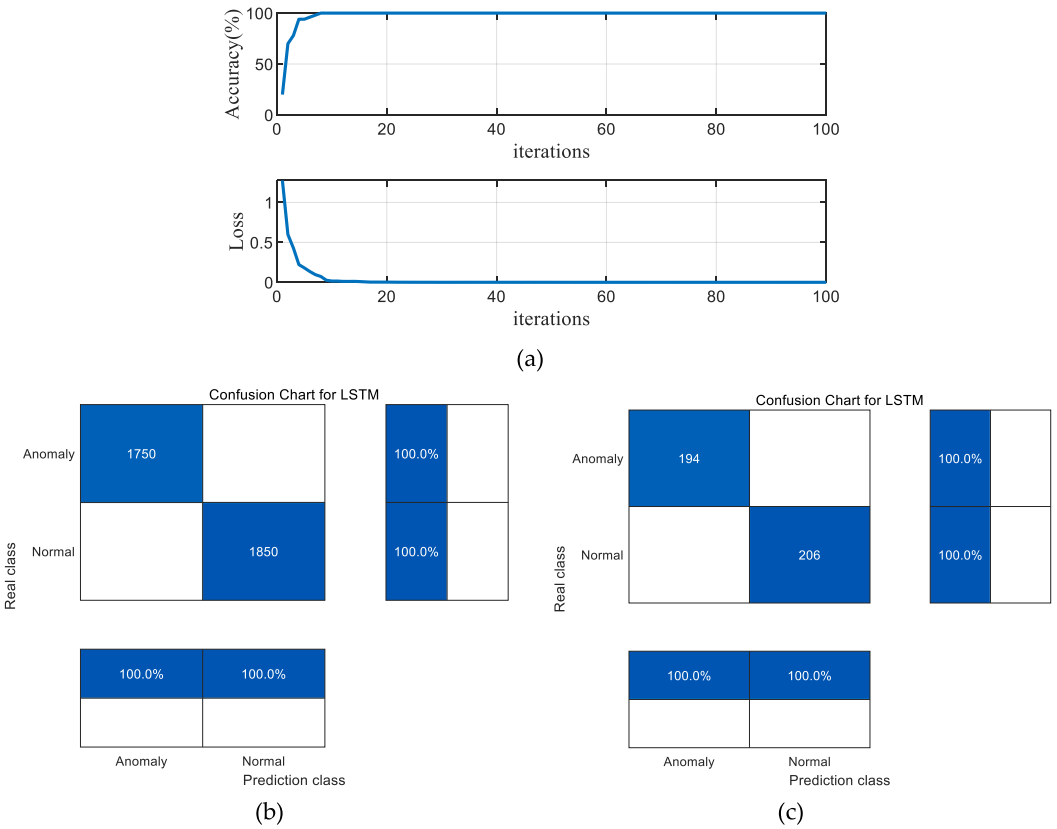

Fig. 9. Results of training and testing by the LSTM model: (a) the algorithm iteration performance; (b) training results; (c) test results.

(1) The BP neural network model adopted a three-layer network structure, with an input number of training and testing samples consistent with the LSTM model. The hidden layer nodes were nodes 6, 7, 8, and 9, and the output layer corresponded to the two classification results. The maximum number of iterations was set to 3,000, the error accuracy was set to 0.001, and the initial value of the learning rate was set to 0.01.
(2) The parameters of the SVM model were configured using a LINER kernel. *C* and *g* are key parameters of the SVM model. To obtain the best parameters, we let *c* and *g* run within a certain range. Using cross-validation, the most accurate values of *c* and *g* were 0.9 and 18, respectively.
(3) The model structure and parameter configuration of the LSTM model are discussed and presented in Section 2.2 and Table 1, respectively. The basic parameters for several PSO algorithms were set as follows: the population size and number of iterations were set at 50 and 1000, respectively. We set c_{max} and c_{min} as 2 and 1.5, respectively. The particle speed was limited between −5 and 5.

The suction detection results of the different models after training are summarised in Fig. 10 and Table 2.

Comparing the accuracy of suction detection in Fig. 10 and Table 2, the overall order of detection accuracy for these six models is: the FFT-GAPSO-LSTM model (100%) > the FFT-APSO-LSTM model (99.2%) > the FFT-PSO-LSTM model (98.75%) > the FFT-LSTM model (98.3%) > the BP neural network model (97.4%) > the SVM model (96.6%). The FFT-GAPSO-LSTM model exhibited the highest accuracy and can be used for suction detection applications.

After the overall comparison, the analysis was conducted from three aspects as follows:

(1) The BP neural network, SVM, and FFT-LSTM models were compared. The FFT-LSTM model had a higher detection accuracy than the individual data in a certain state or the overall data. The BP neural network model had 10 false positives on the overall suction data, whereas the SVM model had as many as 14 false positives, which is dangerous and not allowed in the practical application of centrifugal blood pumps. The FFT-LSTM model had only seven false positives, and after optimising the parameters of the particle swarm optimisation algorithm, it can reach zero false positives, indicating that the FFT-LSTM model is more suitable for application in the suction detection of centrifugal blood pumps.
(2) The results of the first four FFT-LSTM models were compared, one of which was not optimised by the PSO parameters, and the other three were optimised using different PSO algorithms. It can be found that the three FFT-LSTM models optimised using the PSO algorithm have higher accuracy than the FFT-LSTM models without parameter optimisation. The PSO algorithm can effectively improve the convergence and training performance of the FT-LSTM model by optimising its parameters, thereby improving the accuracy of suction detection. The above analysis verifies the necessity of the PSO algorithm for parameter optimisation of LSTM networks.
(3) Finally, the optimisation results of the three particle swarm optimisation algorithms were compared. Compared with the FFT-PSO-LSTM and FFT-APSO-LSTM models, the overall accuracy of the FFT-GAPSO-LSTM model improved by 1.27% and 0.81%, respectively. Based on these data, the improvement may not be significant. But it's worth noting that suction events are extremely dangerous for patients with heart failure, and once suction occurs, irreparable consequences may occur. The FFT-APSO-LSTM model can achieve 100% accuracy, whereas other models have more or less misjudgements. Therefore, it is sufficient to demonstrate the advantages of the GAPSO algorithm for optimising the parameters of the LSTM model.

The above analysis compares the suction effects of different models from both the overall and the three aspects. These results validate the superiority of the FFT-GAPSO-LSTM model for centrifugal blood pump suction detection.

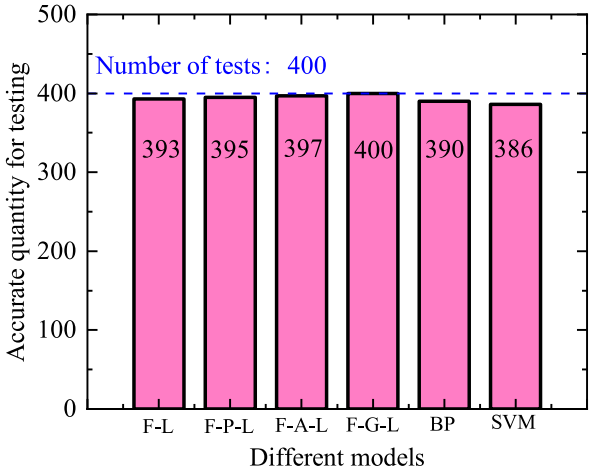

Fig. 10. Accurate number of tests for different models.

Table 2
The suction detection results of different models.

detection model	accuracy (%)		
	normal state	suction state	overall
the FFT-LSTM model	98.7	97.9	98.3
the FFT-PSO-LSTM model	98.5	99.0	98.75
the FFT-APSO-LSTM model	99.3	99.1	99.2
the FFT-GAPSO-LSTM model	100	100	100
the BP neural network model	97.3	97.5	97.4
the SVM model	96.4	96.8	96.6

5. Design and implementation of suction suppression method

5.1. Method design

Suction suppression is necessary after Suction detection. Centrifugal blood pumps satisfy the real-time demand for blood flow by controlling the rotational speed. Suction can occur easily when the speed is excessively high or abnormal. Therefore, when designing suction detection methods, it is necessary to focus on speed modulation. Based on the suction detection method, a suction suppression method was designed in this study; a schematic diagram is shown in Fig. 11.

As shown in Fig. 11, the principle of the suction suppression method is as follows:

(1) If the blood-flow curve detected by the suction detection model is in a normal state, the original state or trend of the rotational speed remains unchanged.
(2) If the detection result of the blood flow curve by the suction-detection model is in a suction state, it indicates that the suction phenomenon has occurred. The motor of the centrifugal blood pump immediately provides a command to continuously reduce the speed until the detection result of the suction-detection model is in a normal state, and the motor stops reducing the speed.

Therefore, it can effectively suppress suction and prevent dangerous events.

5.2. Result analysis

To verify the effectiveness of the suction detection and suppression methods, the method described in Section 4.1, was added to the cardiovascular system, a centrifugal blood pump coupling model was built in MATLAB/Simulink, and simulation research was conducted. The results of the suction suppression are shown in Fig. 12.

Fig. 12 (a) shows the changes in the blood flow of the centrifugal blood pump before and after suction, and Fig. 12 (b) shows the changes in motor speed of the centrifugal blood pump before and after suction. As the motor speed increased, blood flow also increased. When the motor speed reached a certain point, the suction phenomenon occurred, and the periodic fluctuation of the blood flow quickly weakened. At this moment, the suction-detection model detects the suction state and quickly sends instructions to the

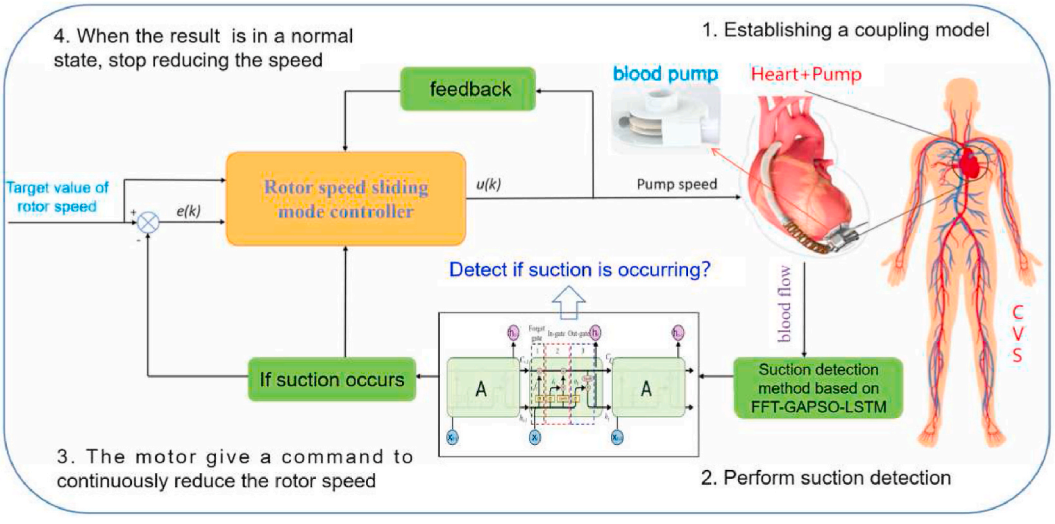

Fig. 11. Schematic diagram of the principle of the suction suppression method.

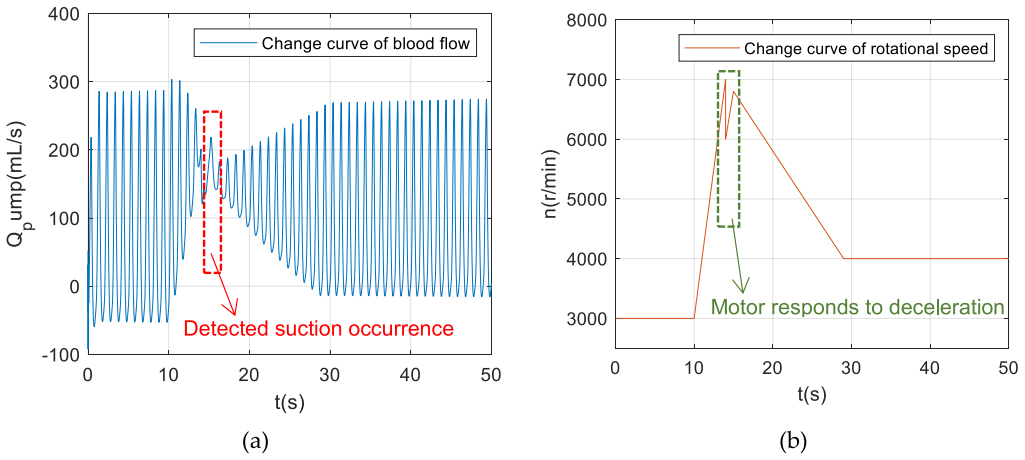

Fig. 12. Results of the suction suppression; (a) blood flow; (b) rotational speed.

motor of the centrifugal blood pump, forcing the motor speed to decrease rapidly, as shown in Fig. 12 (b). Until the blood flow returns to normal, as shown in Fig. 12 (a), the suction detection model detects a transition from the suction state to the normal state and sends another command to the motor. At this point, the centrifugal blood pump motor speed immediately stops decreasing. In this way, the occurrence of suction can be suppressed and subsequent harm to patients can be avoided.

6. Discussion and conclusion

This study combines signal preprocessing, feature extraction, and clustering recognition to design an FFT-GAPSO-LSTM model to detect centrifugal blood pump status. The innovation of this model lies in the application of the GAPSO algorithm and the FFT feature extraction method to the LSTM model, which greatly improves the accuracy of suction detection. Safety is the most important performance of centrifugal blood pumps, which corresponds to the life and health of patients. After implanting a blood pump in patients with heart failure, any minor complications (such as suction) can cause fatal injury. Timely detection of possible suction events can provide valuable information for the suppression and resolution of suction. Therefore, improving the accuracy of suction detection is important. Currently, there are some suction-detection methods available in the market that may, to some extent, detect whether the bleeding pump is in the suction state. However, the accuracy of these methods still needs to be improved because there may be loopholes in their detection. Once suction occurs, it is dangerous, and even a small risk can be fatal. The FFT-GAPSO-LSTM model proposed in this study can achieve a suction detection accuracy of 100%, which can make patients with HF feel comfortable when using it because it will not cause misjudgement. The comparative analysis provided in the Results section verifies the superiority of the FFT-GAPSO-LSTM model. The high accuracy of the model can be explained as follows.

(1) The LSTM model is effective in handling recognition and classification problems, particularly for images. Suction detection in centrifugal blood pumps falls into this category.
(2) After FFT feature extraction, the features of the normal and suction states differed significantly. Therefore, the complexity of the model recognition and detection after feature extraction is significantly reduced. Thus, the training effect of the model is significantly improved.
(3) After optimising the parameters of the GAPSO algorithm, the control parameters of the LSTM model obtained optimal values that significantly improved the convergence performance and training effectiveness of the LSTM model.

Handling the suction problem not only requires ultra-high detection accuracy but also requires corresponding measures to suppress the occurrence of suction after it is detected. The combination of suction detection and suction suppression can achieve normal real-time operation of centrifugal blood pumps. Few studies have reported a complete process that includes these two parts, let alone both simultaneously. We did it. After achieving ultrahigh detection accuracy, we designed a method for suppressing suction based on speed modulation. When suction was detected, the motor of the centrifugal blood pump responded quickly by adjusting the speed of the centrifugal blood pump to its normal state. The simulation results indicate that it is feasible to suppress the suction by modulating the speed. In our control system, a suction-detection algorithm based on the FFT-GAPSO-LSTM model and a suction-suppression algorithm based on speed modulation were integrated. The advantage of this method is that it enables the controller to react quickly, ensuring that the centrifugal blood pump is always in a normal state.

The method of detecting and suppressing centrifugal blood pump suction described in this study is expected to be effective in the clinical application of interventional left ventricular assist devices. A fatal threat of suction in products that are currently on the market exists. The proposed method effectively addresses this problem. However, it also has one limitation, that is, the model must acquire blood flow data in real time and conduct extensive training, which requires the installation of a high-performance controller of a high-

precision flow sensor in the application, which requires a little thought. In short, this study provides a new approach for optimising the control system of centrifugal blood pumps.

In the next step of this research, we will focus on animal experiments, as the current data are based on the simulation of the cardiovascular system and a centrifugal blood pump-coupling model, although the resulting signal has been preprocessed to make it closer to the actual working results. However, centrifugal blood pumps encounter complex environments and unexpected situations after implantation into the human body that are difficult to simulate. Therefore, further experiments must be conducted to verify and analyse these results. Currently, an experimental platform has been established, and a prototype of the centrifugal blood pump has been successfully processed and tested. Our research group will further verify the performance of the centrifugal blood pumps in large-scale animal experiments. We believe that, through repeated verifications and continuous improvement, our heart-pump product will be a step closer to clinical practice.

Data availability statement

Data included in article/supp. material/referenced in article.

Funding

This research was supported by The Institute of Electrical Engineering, CAS(E155420201); The numerical calculations in this study were carried out on the ORISE Supercomputer.

Ethics requirements

Informed consent was not required for this study because this research did not require ethics approval.

Consent to publish

This research did not contains any individual person's data.

CRediT authorship contribution statement

Xin Liu: Writing – review & editing, Writing – original draft, Visualization, Validation, Software, Resources, Methodology, Investigation, Data curation, Conceptualization. **Hongyi Qu:** Writing – review & editing, Validation, Resources, Project administration, Funding acquisition, Conceptualization. **Chuangxin Huang:** Visualization, Software, Data curation. **Lingwei Meng:** Visualization, Software, Methodology. **Qi Chen:** Writing – review & editing, Methodology. **Qiuliang Wang:** Resources, Project administration, Conceptualization.

Declaration of competing interest

The authors declare the following financial interests/personal relationships which may be considered as potential competing interests: Hongyi Qu reports financial support was provided by The Institute of Electrical Engineering, CAS (E155420201).

References

[1] Alberto Esteban-Fernández, Manuel Anguita-Sánchez, J.L. Bonilla-Palomas, et al., Characteristics and in-hospital mortality of elderly patients with heart failure in Spanish hospitals, Journal of Geriatric Cardiology 20 (4) (2023) 247–255.
[2] P. Guo, T. Rao, W. Han, et al., Use of VA-ECMO successfully rescued a trauma patient with fat embolism syndrome complicated with acute heart failure and acute respiratory distress syndrome, World journal of emergency medicine 14 (4) (2023) 332–334.
[3] J. Buber, H.T. Robertson, Cardiopulmonary exercise testing for heart failure: pathophysiology and predictive markers, Heart (British Cardiac Society) 109 (4) (2023) 256–263.
[4] Xin Liu, Hongyi Qu, Lingwei Meng, Chuangxin Huang, Qi Chen, Qiuliang Wang, A sliding mode control of the bearingless permanent magnet slice motor for the blood pump based on the GAPSO, Sci. Rep. 13 (2023) 18929.
[5] Xin Liu, Hongyi Qu, Lingwei Meng, Chuangxin Huang, Qi Chen, Qiuliang Wang, Physiological control of artificial heart pump based on the Hierarchical thought and the fuzzy algorithm, The proceedings of the 10th Frontier Academic Forum of Electrical Engineering (FAFEE2022), Wu Han, Lecture Notes in Electrical Engineering 1048 (2022) 171–179.
[6] Xin Liu, Hongyi Qu, Lingwei Meng, Cong Wang, Qiuliang Wang, A physiological control method based on SMC and GAPSO for artificial heart pumps to maintain pulsatility and avoid regurgitation and suction, J. Med. Biol. Eng. 43 (1) (2022) 42–52.
[7] I. Iwanowski, J. Bckhaus, P. Richardt, et al., A new evaluation Q-factor to Be calculated for suction geometries as a basis for smooth suction in the operating field to ensure the highest possible blood integrity for retransfusion systems, J. Extra Corpor. Technol. (2) (2022) 54.
[8] D.O. Bral, J. Wyrobek, H. Lander, et al., Systolic nonclosure of the mitral valve: two left ventricular assist device patients with pan-cardiac cycle mitral valve opening during shock states, J. Cardiothorac. Vasc. Anesth. 37 (1) (2023) 81–85.
[9] P. Voosen, Global alarm system watches for methane: artificial intelligence-powered scans of satellite data detect leaks of the greenhouse gas, Science 379 (10) (2023) 528.
[10] M. Manimaran, A. Arora, C.A. Lovejoy, et al., Role of artificial intelligence and machine learning in haematology, J. Clin. Pathol. 75 (9) (2022) 585–587.
[11] G. Chen, W.X. Huang, A.D. Ronch, et al., BP neural Network-Kalman filter fusion method for unmanned aerial vehicle target tracking: Proc. IME C J. Mech. Eng. Sci. 237 (18) (2023) 4203–4212.

[12] M. Lather, P. Singh, DDVM: dual decision voting mechanism for brain tumour identification with LBP2Q-SVM type classifier, Int. J. Comput. Vis. Robot 13 (2023) 52–72.
[13] V. Barzegar, S. Laflamme, C. Hu, et al., Ensemble of recurrent neural networks with long short-term memory cells for high-rate structural health monitoring, Mech. Syst. Signal Process. 164 (2022) 108201.
[14] A. Muralikrishna, R.D.C.D. Santos, L.E.A. Vieira, Exploring possibilities for solar irradiance prediction from solar photosphere images using recurrent neural networks, Journal of Space Weather and Space Climate 12 (2022) 19.
[15] A. Eghtesad, K. Germaschewski, M. Knezevic, Coupling of a multi-GPU accelerated elasto-visco-plastic fast Fourier transform constitutive model with the implicit finite element method, Comput. Mater. Sci. 208 (2022), 208.
[16] S. Joseph, E. Amin, RAPPPID: towards generalizable protein interaction prediction with AWD-LSTM twin networks, Bioinformatics (16) (2022) 16.
[17] H.D. Xia, Y. Xue, H.J. Deng, F.J. Liu, Eliminating the disturbance of vegetation information by spectral mixture analysis based on ant colony algorithm, J. Geomechanics 18 (1) (2022) 72–78.
[18] M.M. Moslemi, M. Sadedel, M.M. Moghadam, Optimizing vertical jumping height of single-legged robots with passive TOE joints using the genetic algorithm, Int. J. Humanoid Rob. (1) (2022) 19.
[19] I. Tuba, M. Veinovic, E. Tuba, et al., Tuning convolutional neural network Hyperparameters by bare bones fireworks algorithm[J], Stud. Inf. Control 31 (1) (2022).
[20] T.V. Truong, A. Nayyar, System performance and optimization in NOMA mobile edge computing surveillance network using GA and PSO, Comput. Network. 223 (2023) 109575.
[21] Xin Liu, Hongyi Qu, Lingwei Meng, Qi Chen, Cong Wang, Qiuliang Wang, Sensorless control of the BPMSM for blood pump based on the improved SMO, the improved HFI and the GAPSO algorithm, Measurement 207 (2022) 112305.
[22] J. Du, J. Mi, Z. Jia, et al., Feature extraction and pattern recognition algorithm of power cable partial discharge signal, Int. J. Pattern Recogn. Artif. Intell. 37 (1) (2023).
[23] X. Zhang, M. Shen, X. Li, et al., AABLSTM: a novel multi-task based CNN-RNN deep model for fashion analysis, ACM Trans. Multimed Comput. Commun. Appl 19 (2022) 1–18.
[24] W. Huang, B. Cao, X. Li, et al., Passenger flow prediction for public transportation stations based on spatio-temporal graph convolutional network with periodic components, J. Circ. Syst. Comput. (7) (2022) 31.
[25] H.A. Wen, G.A.P.E. Hong, L.B. Lei, et al., Tool wear prediction based on domain adversarial adaptation and channel attention multiscale convolutional long short-term memory network, J. Manuf. Process. 84 (2022) 1339–1361.
[26] X. Wu, Y. Zhang, X. Zheng, et al., Numerical simulation for suction detection based on improved model of cardiovascular system, Biomed. Signal Process Control 77 (2022) 1–16.
[27] Xin Liu, Hongyi Qu, Lingwei Meng, Cong Wang, Qiuliang Wang, A physiological control method based on SMC and GAPSO for artificial heart pumps to maintain pulsatility and avoid regurgitation and suction, J. Med. Biol. Eng. 43 (1) (2022) 42–52.
[28] Özçelik Yusuf Bahri, A.Y.T.A.C. Altan, Overcoming nonlinear dynamics in diabetic retinopathy classific ation: a robust AI-based model with chaotic swarm intelligence optimization and recurrent long short-term memory, FRACTAL AND FRACTIONAL 8 (7) (2023) 598.
[29] Yag Ilayda, Aytac Altan, Artificial intelligence-based robust hybrid algorithm design and implementation for real-time detection of plant diseases in agricultural environments, BIOLOGY-BASEL 12 (11) (2022) 1732.
[30] Özçelik Yusuf Bahri, Aytaç Altan, Classification of Diabetic Retinopathy by Machine Learning Algorithm Using Entropy-Based Features, ÇANKAYA INTERNATIONAL CONGRESS ON SCIENTIFIC RESEARCH, Ankara, 2023.
[31] Y. Xu, C. Hu, Q. Wu, et al., Research on particle swarm optimization in LSTM neural networks for rainfall-runoff simulation, J. Hydrol. 608 (2022), 608.
[32] E.M. Kuyumani, A.N. Hasan, T. Shongwe, A hybrid model based on CNN-LSTM to detect and forecast harmonics: a case study of an eskom substation in South Africa, Elec. Power Compon. Syst. 51 (8) (2023) 746–760.
[33] D. Pavithra, K. Padmanaban, V. Kumararaja, et al., An in-depth analysis of autism spectrum disorder using optimized deep recurrent neural network, Int. J. Uncertain. Fuzziness Knowledge-Based Syst. 31 (5) (2023) 729–748.
[34] H. Albaqami, G.M. Hassan, A. Datta, MP-SeizNet: a multi-path CNN Bi-LSTM Network for seizure-type classification using EEG[J], Biomed. Signal Process Control 84 (Jul. Pt.1) (2023) 1–12.
[35] Duan Yanjie, L.V. Yisheng, Wang Fei-Yue, Travel time prediction with LSTM neural network, in: 2016 IEEE 19th International Conference on Intelligent Transportation Systems (ITSC), 2016, pp. 1053–1058. Rio de Janeiro, Brazil.
[36] Eliene Andrade Soares, et al., Fourier transform infrared and Raman spectra of the complex cation diethyldithiocarbamate Cr(III) Di-hydrate, [Cr(DDTC)(2)(OH2)(2)](+). UV-Vis spectrum, DFT:B3LYP/6-311G(d,p) structural determination, vibrational and natural bond orbital analysis, J. Mol. Struct. (2022) 1256.
[37] Y.Y. Zhang, L. Zhang, Z.Q. Shang, et al., A new multichannel parallel real-time FFT algorithm for a solar radio observation system based on FPGA, Publ. Astron. Soc. Pac. 134 (1033) (2022).
[38] M.A.T. Rosas, Miguel Robles Pérez, E. Rafael Martínez Pérez, Itineraries for charging and discharging a BESS using energy predictions based on a CNN-LSTM neural network model in BCS, Mexico, Renew. Energy 188 (2022) 1141–1165.
[39] X. Zhang, H. Li, W. Mu, et al., Sensory evaluation and prediction of bulk wine by physicochemical indicators based on PCA-PSO-LSSVM method, J. Food Process. Preserv. 46 (3) (2022).
[40] I. Shafi, A. Aziz, S. Din, et al., Reduced features set neural network approach based on high-resolution time-frequency images for cardiac abnormality detection, Comput. Biol. Med. 145 (2022) 105425.